International Journal of Applied Power Engineering (IJAPE)
Vol. 15, No. 1, March 2026, pp. 195~210
ISSN: 2252-8792, DOI: 10.11591/ijape.v15.i1.pp195-210

Induction motor simultaneous fault diagnosis based on Takagi-Sugeno models

Samira Souri[1], Mohamed Lakhdar Louazene[2], Abdelghani Djeddi[3], Youcef Soufi[3]
[1]Department of Electronics and Telecommunications, Faculty of New Information Technologies and Communication, University Kasdi Merbah-Ouargla, Ouargla, Algeria
[2]Department of Electrical Engineering, Faculty of Applied Sciences, University Kasdi Merbah-Ouargla, Ouargla, Algeria
[3]Department of Electrical Engineering, Faculty of Sciences and Technology, Echahid Cheikh Larbi Tebessi University, Tebessa, Algeria

Article Info

Article history:

Received Feb 13, 2025
Revised Nov 6, 2025
Accepted Nov 28, 2025

Keywords:

Induction motor
Rotor fault
Simultaneous faults
Stator fault
Takagi-Sugeno modeling

ABSTRACT

This article proposes a model-based approach to the concurrent diagnosis of stator and rotor faults in induction motors (IMs) using Takagi–Sugeno (TS) fuzzy models. Fault-free detection is essential to prevent unexpected downtime and economic loss in industrial applications. The study first develops a dynamic model of the IM in the synchronized reference frame with the rotor under healthy and faulty operations. Different fault conditions like stator inter-turn short circuits, defective rotor bars, and combination thereof are considered. A TS model for every case is developed based on the precise nonlinear model. Simulation outcomes prove the validity of the new models in simulating the dynamic response of the motor under faulty operating modes. The residual signals are used to compare the performance of the model in fault isolation. The proposed method offers a classification that inherently separates between fault types. Such a contribution presents an efficient real-time fault detection and predictive maintenance facility, which renders it suitable for hardware-in-the-loop application in intelligent drive systems.

Corresponding Author:

Samira Souri
Department of Electronics and Telecommunications
Faculty of New Information Technologies and Communication, University Kasdi Merbah-Ouargla
Ouargla, Algeria
Email: souri.samira@univ-ouargla.dz

1. INTRODUCTION

Induction motors (IMs) are ubiquitous actuators in industrial drives, where unexpected outages incur high operational costs. While single-fault diagnosis has been extensively studied, diagnosing simultaneous stator–rotor faults remain particularly challenging due to the interaction of their electrical signatures, which vary with load and speed, and can mask each other. For a solution to be usable in measurement and control applications, it should rely primarily on routinely available electrical quantities, such as stator currents and voltages and estimated speed or torque; it should operate under variable load and during transients; it should distinguish between fault types—such as stator inter-turn short circuits and broken rotor bars—and fault severity; and it should remain computationally efficient for real-time or hardware-in-the-loop use. Classical spectrum or Park-vector methods degrade when multiple faults co-exist or when the operating point drifts, whereas purely data-driven classifiers may struggle to generalize beyond trained conditions. This motivates a model-based yet tractable approach that captures the IM's nonlinear behaviour while enabling simple residual generation for diagnosis.

IMs are ubiquitous actuators in industrial drives, where unexpected outages incur high operational costs. While single-fault diagnosis has been extensively studied, simultaneous stator–rotor faults remain particularly challenging because their electrical signatures interact, vary with load and speed, and can mask one another. For a solution to be usable in measurement and control applications, it should rely primarily on routinely available electrical quantities, such as stator currents and voltages and estimated speed or torque; it should operate under variable load and during transients; it should distinguish between fault types—such as stator inter-turn short circuits and broken rotor bars—and fault severity; and it should remain computationally efficient for real-time or hardware-in-the-loop use. Classical spectrum or Park-vector methods degrade when multiple faults co-exist or when the operating point drifts, whereas purely data-driven classifiers may struggle to generalize beyond trained conditions.

Several model-based and hybrid techniques have emerged to overcome these issues. Classical signal-based methods such as Park's vector [1], motor current signature analysis (MCSA) [2], and fast Fourier transform [3] offer useful detection tools but suffer from reduced sensitivity under multiple or evolving fault conditions [4], [5]. AI-based methods using neural networks [6]-[9] and support vector machines [10] have shown strong classification abilities but remain limited by training data generalization and computational load.

This motivates a model-based yet tractable approach that captures the IM's nonlinear behaviour while enabling simple residual generation for diagnosis [11]-[13]. Fault estimation has also been addressed in current research using fuzzy observers for employment in Takagi–Sugeno models. Ouarid *et al*. [14], for example, described the application of a fuzzy observer design to fault and state estimation of TS singular systems and demonstrated how fuzzy logic can improve system diagnosis and robustness in complex industrial setups.

Further, Aitdaraou *et al*. [15] proposed an implicit TS observer structure for fault estimation improvement in line with Sugeno and Tanaka's original theory [16]. These TS observers are suitable for real-time applications in nonlinear systems like IMs [17], [18]. Their approach highlights the observer-based fault detection robustness of the TS formalism, supporting control-oriented modeling approach that we propose in this paper.

The literature on IM fault diagnosis has evolved along several main lines. Spectrum and Park-vector methods, pioneered by Nandi *et al*. [19] and Bellini *et al*. [20], relied on motor current signature analysis (MCSA) to detect broken rotor bars under steady slip, while Park-vector and extended Park-vector approaches [1] improved stator-fault sensitivity. However, these techniques suffer from spectral or trajectory overlap when faults co-exist or when the operating point changes.

To address these limitations, wavelet-based methods such as those in [20]-[22] have been proposed to capture transient fault signatures. Benbouzid and Kliman [22] analyzed mechanical faults using wavelet packet decomposition, and Yarymbash *et al*. [21] coupled wavelets with ANFIS for improved detection. Hybrid strategies such as Hilbert–Huang transform with SVM [10], and DWT with machine learning [23], further enhance accuracy under varying conditions. Nevertheless, their high computational cost and tuning complexity restrict practical deployment [24], [25].

IMs are extensively used in industrial applications due to their robustness and simplicity. However, unexpected failures—especially simultaneous faults affecting both the stator and rotor—can result in severe operational downtime and financial loss. The early and accurate diagnosis of such faults is essential to ensure reliability and efficiency [3], [4], [26].

Despite all these advances, the majority of available literature focuses on isolated faults or sensor/actuator faults. Simultaneous electrical rotor–stator faults, particularly under time-varying load or transient, are not yet properly addressed. This is an inherent deficiency, as the coupling among such faults generates complex signatures that are detrimental to the performance of traditional diagnostic methods.

In a bid to bridge this, the present work proposes a new diagnostic method through Takagi–Sugeno (TS) fuzzy models for simultaneous faults of induction motors (IMs). The present paper offers a generic TS model formulation that has the ability to handle both rotor and stator faults within a single unified mathematical framework. The approach is verified through extensive simulations for loaded and dynamic operation conditions, e.g., simultaneously present faults. Furthermore, the new methodology has increased fault detection robustness by tapping into fuzzy interpolation techniques that prevent the need for extensive dataset-dependent tuning and provide greater model flexibility across varying operating regimes.

The originality of this work lies in its combined Takagi–Sugeno fuzzy modeling architecture with simultaneous capability to manage rotor and stator electrical faults, an under-researched area in previous work. Unlike conventional methodologies that construct isolated fault configurations or sensor/actuator faults, our strategy portrays the complex interactions of faults occurring simultaneously using sub-linear TS arrangements. The system is designed for real-time operation using an efficient computationally simulation platform in MATLAB/Simulink. The model also supports dynamic performance for transient and loaded

operation that is typically not considered. The structure of the simulation environment supports the modularity of injecting faults of different types and visualization of the diagnostic quantities such as torque disturbance, speed fluctuation, and current asymmetries. To validate the proposed method, fault diagnosis simulations were carried out in MATLAB/Simulink for both pseudo-linear representations with variable parameters and TS fuzzy representations of the studied IM.

The remainder of this paper is structured to demonstrate the development and applicability of the method proposed. In section 2, the proposed method is introduced. In section 3, the method is presented, including the Takagi–Sugeno fuzzy modelling framework as well as the modelling and simulation of the induction motor in both healthy and faulty conditions, where the healthy model serves as the reference for fault detection. Section 4 addresses the co-occurrence of stator and rotor faults—an often overlooked but significant case—and examines the motor behavior using both conventional state-space and TS-based models, supported by simulation results and discussion. The MATLAB/Simulink diagnostic environment architecture and implementation are also presented. Finally, section 5 concludes the paper briefly by recapitulating the contributions made and elaborating on the applicability of the presented method to real-time fault detection systems.

2. THE PROPOSED METHOD

The fault detection of the induction motors (IMs) with simultaneous stator and rotor faults is a complicated task with intertwined electrical and mechanical behavior impacts of the faults. Traditional diagnosis techniques have a tendency of catching overlapping fault signatures, especially under non-stationary operating conditions. To overcome this issue, the proposed method employs a systematic and generalized modeling paradigm based on the Takagi–Sugeno (TS) fuzzy formalism. The method begins with establishing proper nonlinear state-space models of the IM for different fault situations including the normal situation, stator fault, rotor fault, and combined fault. The models are then transformed into TS fuzzy models using sector nonlinearity techniques, allowing complex dynamics to be decomposed into a set of local linear submodels. Each local model is linked with an individual operating area, dynamically weighted by membership functions that consider dynamic variations in system states. The approach enables the creation of an interpretable diagnostic system capable of handling nonlinearities and fault couplings. Here we describe the modeling strategy, the inclusion of faults, TS conversion process, and the overall simulation structure utilized to probe the method under a range of dynamic and loaded scenarios.

3. METHOD

This part describes the modeling strategy employed to model the induction motor (IM) operation under different operating conditions, including healthy and faulty conditions. A mathematical representation is first obtained in the rotor reference frame in order to facilitate a consistent description of electrical and mechanical dynamics. The models are then developed in state-space form so that they can be simulated and fault detection based on observers can be facilitated. Moreover, the Takagi–Sugeno fuzzy modeling framework is also introduced as an approach to approximating nonlinearity at no computational tractability cost.

3.1. Takagi-Sugeno fuzzy models

The Takagi-Sugeno model is based on the use of a set of simple structure sub-models, each sub-model describing the behaviour of the system in a particular "operating zone". These sub-models are then used to describe the overall dynamic behaviour of the system using non-linear functions (weight functions) defining the contribution of each sub-model. The ability of Takagi-Sugeno to represent or approximate the dynamic behaviour of a real system has been widely recognized. Indeed, on the one hand, they offer the possibility of describing very complex nonlinear behaviours with a simple structure inspired by linear models. On the other hand, their particular structure allows the extension of certain results obtained within the framework of linear systems.

TS model can be obtained by using the convex polytopic transformation which leads to a number of local linear time invariant (LTI) models depending on number of nonlinearities contained in the system [18]. TS representation can be written as (1).

$$\begin{cases} \dot{x}(t) = \sum_{i=1}^{r} h_i\big(z(t)\big)\{A_i x(t) + B_i u(t)\} \\ \quad y(t) = \sum_{i=1}^{r} h_i\big(z(t)\big)\{C_i x(t)\} \end{cases}, \tag{1}$$

Where $h_i\big(z(t)\big) \geq 0$ have the property of convex sum:

$$\forall t \geq 0 \sum_{i=1}^{r} h_i(z(t)) = 1$$

$z(t)$ are the premise variables (dependent on the input and/or the state of the system); r is the number of rules; $x(t) \in R^n$, $y(t) \in R^p$, and $u(t) \in R^m$ represent the state vector, the output vector, and the input vector, respectively; and $A_i \in R^{n\times n}$, $B_i \in R^{n\times m}$, and $C_i \in R^{p\times n}$ represent respectively the state matrix, the system input matrix, and the output matrix [18].

This section introduces the general modeling strategy based on the Takagi–Sugeno fuzzy inference system. The purpose is to construct a flexible nonlinear model capable of describing both healthy and faulty dynamics of the induction motor. The proposed formulation ensures modularity and ease of adaptation to different fault scenarios, which will be detailed in the following sections.

3.2. Modelling of the induction motor (IM) in the frame of reference linked to the rotor in healthy case

The model of the IM in park frame is given by (2) and (3). The expression of the torque T_e in Park's frame is as (4). The mechanical speed equation is given by (5).

$$\begin{cases} U_{dqs} = R_s i_{dqs} + \frac{d}{dt}\varphi_{dqs} + \omega p\left(\frac{\pi}{2}\right)\varphi_{dqs} \\ 0 = R_r i_{dqr} + \frac{d}{dt}\varphi_{dqr} \end{cases} \quad (2)$$

$$\begin{cases} \varphi_{dqs} = L_f i_{dqs} + (L_m + L_f) i_{dqr} \\ \varphi_{dqr} = L_m(i_{dqs} + i_{dqr}) \end{cases} \quad (3)$$

$$T_e = p(\varphi_{dr} i_{qs} - \varphi_{qr} i_{ds}) \quad (4)$$

$$\frac{d\omega}{dt} = \frac{p^2}{J}(i_{qs}\varphi_{dr} - i_{ds}\varphi_{qr}) - \frac{f}{J}\omega - \frac{p}{J}T_r \quad (5)$$

Where: R_s and R_r are respectively the stator and rotor resistance; L_f and L_m are rotor leakage inductance and mutual inductances between the stator and rotor; φ_{dqs} and φ_{dqr} are stator and rotor flux reference frame *(d, q)*; T_e and T_r are electromagnetic torque of IM and resistant torque; J is machine inertia; f is Viscous friction coefficient; ω is speed rotation; and p is number of pole pairs.

3.2.1. State-space representation in healthy case

This section presents the modeling of the healthy induction motor system (denoted M1), which serves as the baseline reference for comparison with fault-induced behaviors. The goal is to establish the nominal behavior against which anomalies can be detected using the TS fuzzy framework. The state space model of the IM is obtained by associating the stator and rotor currents state vector. IM can be described by (6) [19]:

$$\begin{cases} \dot{x}(t) = A(\omega)\cdot x(t) + B(t)\cdot u(t) \\ y(t) = C\cdot x(t) \end{cases} \quad (6)$$

with: $x(t) = [i_{ds} \quad i_{qs} \quad \varphi_{dr} \quad \varphi_{qr}]^T$, $u(t) = [U_{ds} \quad U_{qs}]^T$, and $y(t) = [i_{ds} \quad i_{qs}]^T$.

$$A(\omega) = \begin{bmatrix} -\frac{R_s+R_r}{L_f} & \omega & \frac{R_r}{L_m L_f} & \frac{\omega}{L_f} \\ -\omega & -\frac{R_s+R_r}{L_f} & -\frac{\omega}{L_f} & \frac{R_r}{L_m L_f} \\ R_r & 0 & -\frac{R_r}{L_m} & 0 \\ 0 & R_r & 0 & -\frac{R_r}{L_m} \end{bmatrix}, B = \begin{bmatrix} \frac{1}{L_f} & 0 \\ 0 & \frac{1}{L_f} \\ 0 & 0 \\ 0 & 0 \end{bmatrix}, C = \begin{bmatrix} 1 & 0 & 0 & 0 \\ 0 & 1 & 0 & 0 \end{bmatrix}.$$

3.2.2. Simulation results in healthy case

The used IM parameters for simulation are: rated power 1.1 kW, stator resistance $R_s = 9.81\,\Omega$, Rotor resistance $R_r = 3.83\,\Omega$, magnetizing inductances $L_m = 0.436\,H$, global leakage inductance referred to stator $L_f = 0.0762H$, and number of pole pairs $p = 2$ [20]. During the simulations, a resistive torque equal to 3.5 N.m is applied to the IM at time t = 0.7 s. The carried-out waveforms correspond well to normal operation of the IM at the nominal voltage with a balanced sinusoidal power supply. Figure 1 illustrates respectively the evaluation of the speed, torque, and currents waveforms. After a transient regime due to the

starting phase, the last waveforms converge to the nominal values after 0.5 s. We notice that, at the beginning a series of high amplitude oscillations are damped during the acceleration of the IM and at the end of the starting speed 0.7 s. The torque reaches its maximum value, and then attenuates to reach its resistive value and the currents zoom show that the three phase currents are well balanced.

The speed waveform stabilizes at approximately 150 rad/s after the transient period. The torque reaches a peak value of 4 N.m at t = 0.7 s, before stabilizing at 3.5 N.m. The three-phase currents converge to nominal values with balanced magnitudes of around 5 A after the initial oscillations. We notice that the passage from unloaded regime to the loaded one at time t = 0.7 s is established without oscillations, and with a very low overtaking.

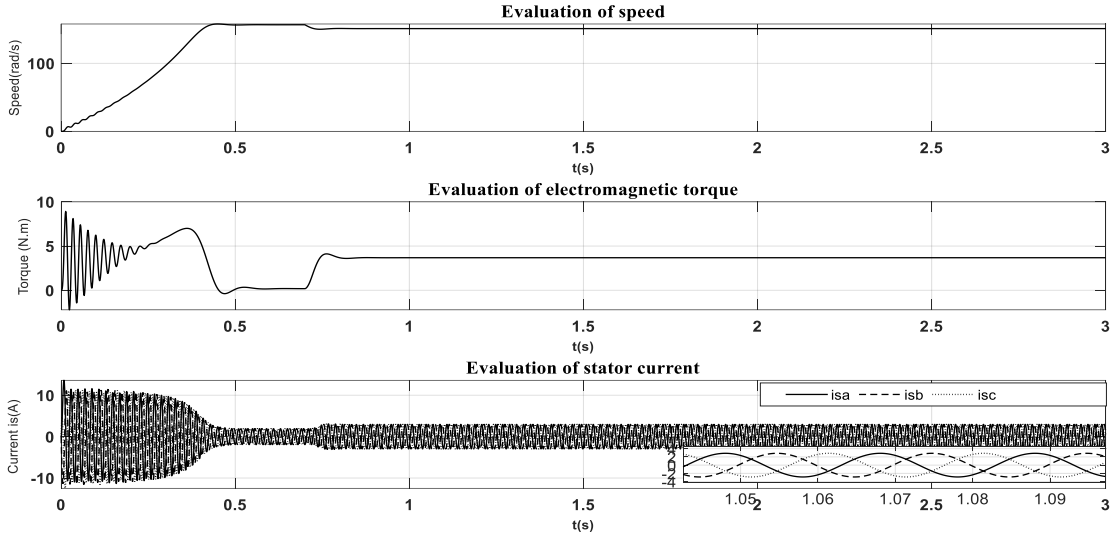

Figure 1. Speed, torque, and currents waveforms under load T_r = 3.5 N.m in healthy case

3.2.3. Representation with Takagi–Sugeno models in healthy case

Following to (6), we notice that the matrix control B and the matrix observation C, are constants, and the matrix state A depend on the speed. Which represents the nonlinearity: $z(t) = \omega$. TS matrices of the studied IM are given as follows:

$$A_1 = \begin{bmatrix} -\frac{R_s+R_r}{L_f} & W & \frac{R_r}{L_m L_f} & \frac{W}{L_f} \\ -W & -\frac{R_s+R_r}{L_f} & -\frac{W}{L_f} & \frac{R_r}{L_m L_f} \\ R_r & 0 & -\frac{R_r}{L_m} & 0 \\ 0 & R_r & 0 & -\frac{R_r}{L_m} \end{bmatrix}, \quad A_2 = \begin{bmatrix} -\frac{R_s+R_r}{L_f} & w & \frac{R_r}{L_m L_f} & \frac{w}{L_f} \\ -w & -\frac{R_s+R_r}{L_f} & -\frac{w}{L_f} & \frac{R_r}{L_m L_f} \\ R_r & 0 & -\frac{R_r}{L_m} & 0 \\ 0 & R_r & 0 & -\frac{R_r}{L_m} \end{bmatrix},$$

$$B_1 = B_2 = B, \quad C_1 = C_2 = C.$$

3.2.4. Simulation results based on TS models

To validate the proposed TS model, MATLAB/Simulink package is used to simulate the behaviour of the considered motor. Figure 2 illustrates the evaluation of speed, electromagnetic torque, and stator currents which converge to their real values. The electromagnetic torque stabilizes at 3.5 N.m, while the speed converges to 150 rad/s. The stator currents show balanced sinusoidal patterns with amplitudes of approximately 5 A.

3.3. Modelling of the IM with stator fault in the frame of reference linked to the rotor

This section describes the construction of the stator and rotor fault models (M2 and M3). These models are developed by modifying the healthy system to reflect physical fault signatures, while preserving compatibility with the TS-based interpolation framework. All parameter changes and simulation settings are aligned with real fault conditions in industrial motors. The model of the studied motor in the presence of short circuit between turns fault in the stator can be obtained using the representation Figure 3 where n_{cc} represents the number of faulty turns [19].

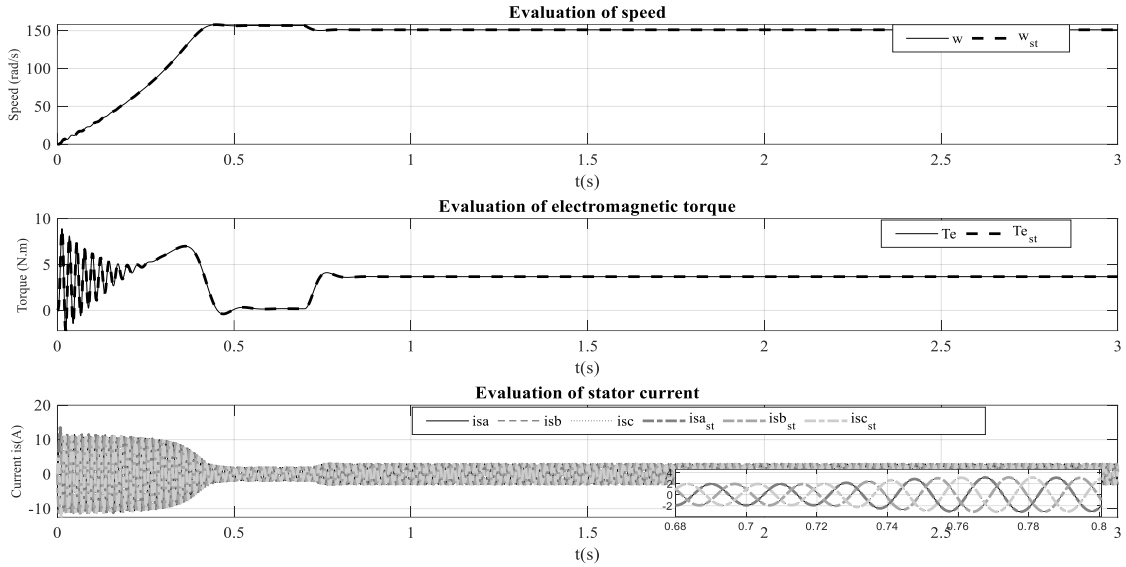

Figure 2. Speed, torque, and currents waveforms-based TS models under load Tr = 3.5 N.m in healthy case

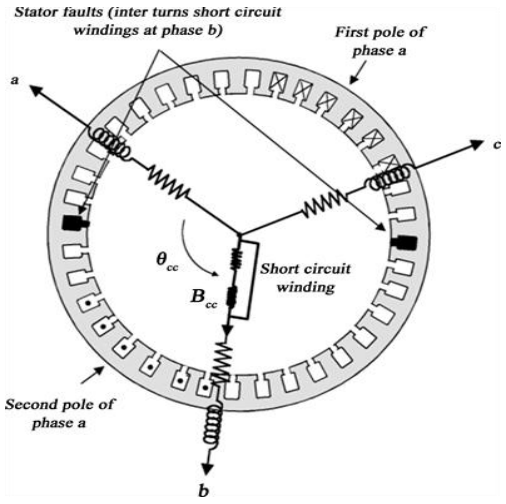

Figure 3. Short circuit of turns on the bs phase of the stator

For fault isolation, it is important to introduce two parameters. The electrical angle noted θ_{cc}, identifying the short-circuited winding with respect to the reference axis α_s. The noted short-circuit report n_{cc}, equal to the ratio of the number of short-circuited turns to the total number of turns in a real stator phase in healthy case. The R_{cc} which represents the short circuit between turn is given by the following equation [19]. IM stator faults state space representation linked to the rotor. The IM stator faults state space representation linked to the rotor are given by (7), with: $n_{cc} = \frac{N_{cc}}{n_s}$.

$$R_{cc} = n_{cc} \cdot R_s \tag{7}$$

Park IM equations linked to the rotor are given by (8)-(10).

$$\begin{cases} U_{dqs} = R_s i'_{dqs} + \frac{d}{dt}\varphi_{dqs} + \omega p\left(\frac{\pi}{2}\right)\varphi_{dqs} \\ 0 = R_r i'_{dqr} + \frac{d}{dt}\varphi_{dqr} \end{cases} \tag{8}$$

$$\begin{cases} \varphi_{dqs} = L_f i'_{dqs} + (L_m + L_f) i_{dqr} \\ \varphi_{dqr} = L_m\left(i'_{dqs} + i'_{dqr}\right) \end{cases} \tag{9}$$

$$\begin{cases} i_{dqs} = i_{dqs}^{'} + i_{dqcc} \\ i_{dqcc} = \frac{2}{3}\frac{n_{cc}}{R_s} P(-\theta)Q(\theta_{cc})P(\theta)U_{dqs} \end{cases} \quad (10)$$

3.3.1. State-space representation with stator fault

The IM stator faults state-space representation linked to the rotor is given by (11). This representation describes the system behavior under rotor-linked stator faults.

$$\begin{cases} \dot{x}(t) = A(\omega) \cdot x(t) + B \cdot u(t) \\ y(t) = C \cdot x(t) + D \cdot u(t) \end{cases}, \quad (11)$$

With $x(t) = [i'_{ds} \quad i'_{qs} \quad \varphi_{dr} \quad \varphi_{qr}]^T$, $u(t) = [U_{ds} \quad U_{qs}]^T$, and $y(t) = [i_{ds} \quad i_{qs}]^T$.

$$A(\omega) = \begin{bmatrix} -\frac{R_s+R_r}{L_f} & \omega & \frac{R_r}{L_m L_f} & \frac{\omega}{L_f} \\ -\omega & -\frac{R_s+R_r}{L_f} & -\frac{\omega}{L_f} & \frac{R_r}{L_m L_f} \\ R_r & 0 & -\frac{R_r}{L_m} & 0 \\ 0 & R_r & 0 & -\frac{R_r}{L_m} \end{bmatrix}, \; B = \begin{bmatrix} \frac{1}{L_f} & 0 \\ 0 & \frac{1}{L_f} \\ 0 & 0 \\ 0 & 0 \end{bmatrix}, \; C = \begin{bmatrix} 1 & 0 & 0 & 0 \\ 0 & 1 & 0 & 0 \end{bmatrix}$$

$$D = \sum_{k=1}^{3} \frac{2}{3}\frac{n_{cck}}{R_s} P(-\theta)Q(\theta_{cck})P(\theta), \quad (12)$$

$$Q(\theta_{cck}) = \begin{bmatrix} cos(\theta_{cck})^2 & cos(\theta_{cck}).sin(\theta_{cck}) \\ cos(\theta_{cck}).sin(\theta_{cck}) & sin(\theta_{cck})^2 \end{bmatrix}, P(\theta) = \begin{bmatrix} cos(\theta) & -sin(\theta) \\ sin(\theta) & cos(\theta) \end{bmatrix}.$$

3.3.2. Simulation results

Figure 4 illustrates the evaluation of the speed, torque, and currents waveforms in the presence of 5%, 15%, and 25% short circuit between turns in the stator under 3.5 N.m applied to the IM at t = 0.7 s. Also, at t = 1 s, a short circuit fault between turns equal to 5% and 15% which represents respectively, a n_{cc} = 23 turns and n_{cc} = 69 turns is provoked, followed by short circuit equivalent to a short-circuit of 25% (n_{cc} =116 turns) at t = 1.5 s and t = 2 s is respectively simulated. We notice that during the shortened turns in the study state, the stator currents amplitude changes due to magnetic coupling which leads to an increased oscillation in the speed and torque. At 5% short circuit, the current amplitude rises to 6 A, increasing to 8 A at 15% fault and 10 A at 25% fault. The oscillation in torque reaches 4 N.m, 5 N.m, and 6 N.m for 5%, 15%, and 25% faults, respectively.

3.3.3. Takagi–Sugeno models of IM with stator fault

As shown in (11), we notice that the matrices *B* and *C* in case of stator fault using TS representation are constants where, the matrix state A depend on the speed, which represents the only nonlinearity: *z(t) = ω*. The matrices of the system are given as:

$$A_1 = \begin{bmatrix} -\frac{R_s+R_r}{L_f} & W & \frac{R_r}{L_m L_f} & \frac{W}{L_f} \\ -W & -\frac{R_s+R_r}{L_f} & -\frac{W}{L_f} & \frac{R_r}{L_m L_f} \\ R_r & 0 & -\frac{R_r}{L_m} & 0 \\ 0 & R_r & 0 & -\frac{R_r}{L_m} \end{bmatrix}, A_2 = \begin{bmatrix} -\frac{R_s+R_r}{L_f} & w & \frac{R_r}{L_m L_f} & \frac{w}{L_f} \\ -w & -\frac{R_s+R_r}{L_f} & -\frac{w}{L_f} & \frac{R_r}{L_m L_f} \\ R_r & 0 & -\frac{R_r}{L_m} & 0 \\ 0 & R_r & 0 & -\frac{R_r}{L_m} \end{bmatrix},$$

$$B_1 = B_2 = B, \;\; C_1 = C_2 = C, D_1 = D_2 = D.$$

3.3.4. Simulation results based on TS models

Figure 5 shows respectively the evaluation of the speed, torque, and currents waveforms in the presence of the stator fault based on TS models. We notice that the quantities (torque, speed, and currents with stator fault) converge towards their real values. The currents stabilize at around 5 A under normal operating conditions, while the torque oscillations increase from 3.5 N.m to 4 N.m as the fault level increases.

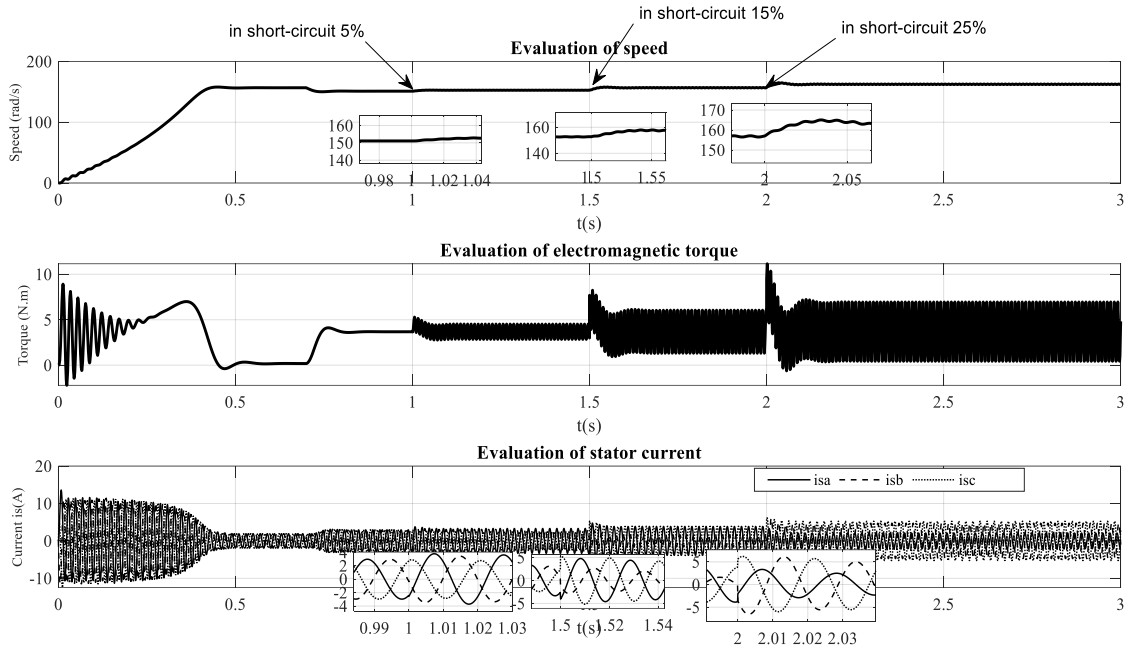

Figure 4. Speed, torque, and currents waveforms in short circuit fault under load T_r = 3.5 N.m

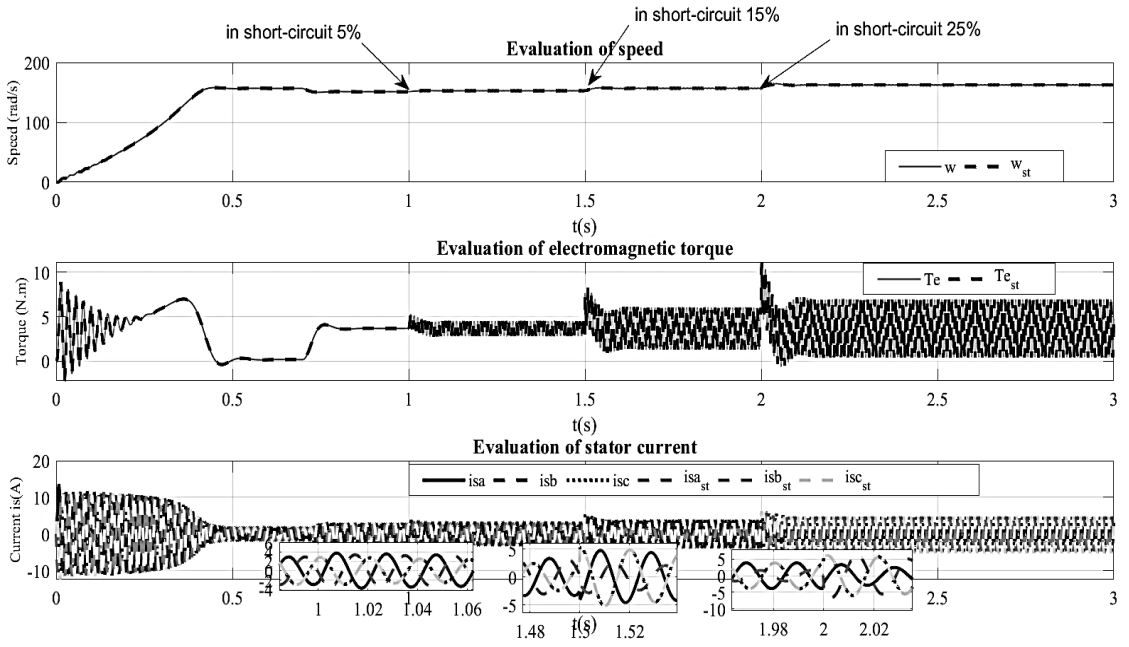

Figure 5. Speed, torque, and currents waveforms in stator fault-based TS models

3.4. Modelling of the IM with rotor fault in the rotor frame

This sub-section describes for the simultaneous fault models (M4 and M5), which represent the simultaneous presence of rotor and stator faults. They are used to test the robustness of the TS fuzzy approach under more adverse fault couplings. The simulation design and the timing for fault activation are outlined with a view to ensuring total reproducibility. Figure 6 illustrates the conventional modelling of the rotor by elementary dipoles with a broken bar. It is assumed that the rotor in the presence of a fault is equivalent to a rotor in free of fault case, to which we add an additional winding traversed by a fictitious fault current [21].

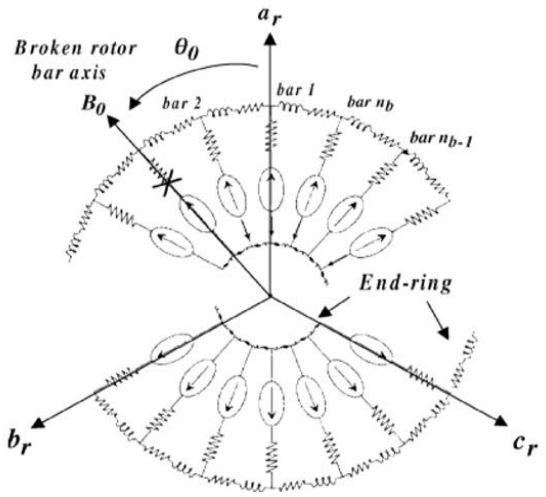

Figure 6. IM rotor broken bars circuit

3.4.1. Modelling of broken rotor bar faults

Figure 6 represents the equivalent electrical circuit of the IM with broken bar fault. In this study, we focused on modelling the faults based on changes in resistance, particularly for rotor faults. The choice to neglect inductance changes was made because, for the studied scenarios, resistance variations dominated the fault dynamics. However, in more severe fault cases or under different operating conditions, inductance changes might have a significant impact, and accounting for them would lead to a more accurate and comprehensive model.

The bar ruptures at the rotor amount to a simple resistive quadrupole R_{fault} placed in series with the rotor resistance. The expression of the rotor equivalent resistance matrix is then obtained as (13).

$$[R_{eq}] = [R_r] + [R_{fault}] = [R_r] - \frac{\alpha}{1-\alpha} Q(\theta_0).[R_r] \tag{13}$$

With $\alpha = \frac{2}{3}\eta_0$, $[R_r] = R_r \begin{bmatrix} 1 & 0 \\ 0 & 1 \end{bmatrix}$, and $Q(\theta_0) = \begin{bmatrix} cos(\theta_0)^2 & \cos(\theta_0).sin(\theta_0) \\ \cos(\theta_0).sin(\theta_0) & sin(\theta_0)^2 \end{bmatrix}$.

A fictitious phase therefore consists of $\eta_b/3$ bars. For n_{bc} broken bars on a phase, the expression of the fault report η_0 is given by [21]: $\eta_0 = 3n_{bc}/n_b$. In healthy case (factor $\alpha = 0$), the resistance R_{fault} becomes zero. When the factor α is non-zero, the resistance R_{fault} introduces an imbalance in the rotor sizes and the coupling terms on the two d and q axes of the rotor.

3.4.2. State-space representation with rotor fault

The model of the studied motor under rotor broken bar fault is described by the state-space representation as (14) and (15). This representation characterizes the motor behavior when a rotor broken bar fault occurs.

$$\begin{cases} \dot{x}(t) = A(\omega).x(t) + B(t).u(t) \\ y(t) = C.x(t) \end{cases} \tag{14}$$

With $x(t) = [i_{ds} \quad i_{qs} \quad \varphi_{dr} \quad \varphi_{qr}]^T$, $u(t) = [U_{ds} \quad U_{qs}]^T$, and $y(t) = [i_{ds} \quad i_{qs}]^T$.

$$A(\omega) = \begin{bmatrix} -\left([R_s] + [R_{eq}]\right).L_f^{-1} - \omega.P\left(\frac{\pi}{2}\right) & \left([R_{eq}].L_m^{-1} - \omega.P\left(\frac{\pi}{2}\right)\right).L_f^{-1} \\ [R_{eq}] & -[R_{eq}].L_m^{-1} \end{bmatrix}, B = \begin{bmatrix} \frac{1}{L_f} & 0 \\ 0 & \frac{1}{L_f} \\ 0 & 0 \\ 0 & 0 \end{bmatrix},$$

$$C = \begin{bmatrix} 1 & 0 & 0 & 0 \\ 0 & 1 & 0 & 0 \end{bmatrix}, [R_{eq}] = [R_r].(I - \frac{\alpha}{1-\alpha} Q(\theta_0)) \tag{15}$$

3.4.3. Simulation results in the presence of rotor faults

First, The IM is started without load until t = 0.7 s, followed by applying a resistive torque equal to 3.5 N.m. where the speed drops to 151.1 rad/s, followed by the provocation of the rotor broken bars at t = 1 s, we notice the appearance of oscillation in speed, torque, and currents waveforms (Figure 7) and their zoom and verifies the modulation of the stator current envelope for one rotor broken bar. The broken of two bars is applied at t = 2 s. We remark, the increasing of the amplitude oscillations in speed, torque, and currents waveforms. In the case of rotor faults, the torque oscillations increase from 3 N.m to 4 N.m as a second rotor bar fault is introduced.

3.4.4. Takagi–Sugeno models of IM with rotor fault

Following to (14), we notice that the matrices *B* and *C* in case of stator fault using TS representation are constants where, the matrix state A depend on the speed, which represents the only nonlinearity: *z(t) = ω.* The matrices of the system are given as:

$$A_1 = \begin{bmatrix} -\left([R_s] + [R_{eq}]\right).L_f^{-1} - W.P(\frac{\pi}{2}) & \left([R_{eq}].L_m^{-1} - W.P\left(\frac{\pi}{2}\right)\right).L_f^{-1} \\ [R_{eq}] & -[R_{eq}].L_m^{-1} \end{bmatrix}$$

$$A_2 = \begin{bmatrix} -\left([R_s] + [R_{eq}]\right).L_f^{-1} - w.P(\frac{\pi}{2}) & \left([R_{eq}].L_m^{-1} - w.P\left(\frac{\pi}{2}\right)\right).L_f^{-1} \\ [R_{eq}] & -[R_{eq}].L_m^{-1} \end{bmatrix}$$

$$B_1 = B_2 = B, \quad C_1 = C_2 = C$$

3.4.5. Simulation results based on TS models

Figure 8 represents, respectively, the behaviour of the torque, real speed, and the stator current in TS form with the presence of rotor faults. At in t = 1 s and at t = 2 s, one bar breaks and two broken bars are provoked in simulation, and the amplitude of observed oscillations were increased when the number of broken bars is increased and the torque, speed and current quantities converge towards their real values. The amplitude of torque oscillations increases further, confirming the increase in fault severity.

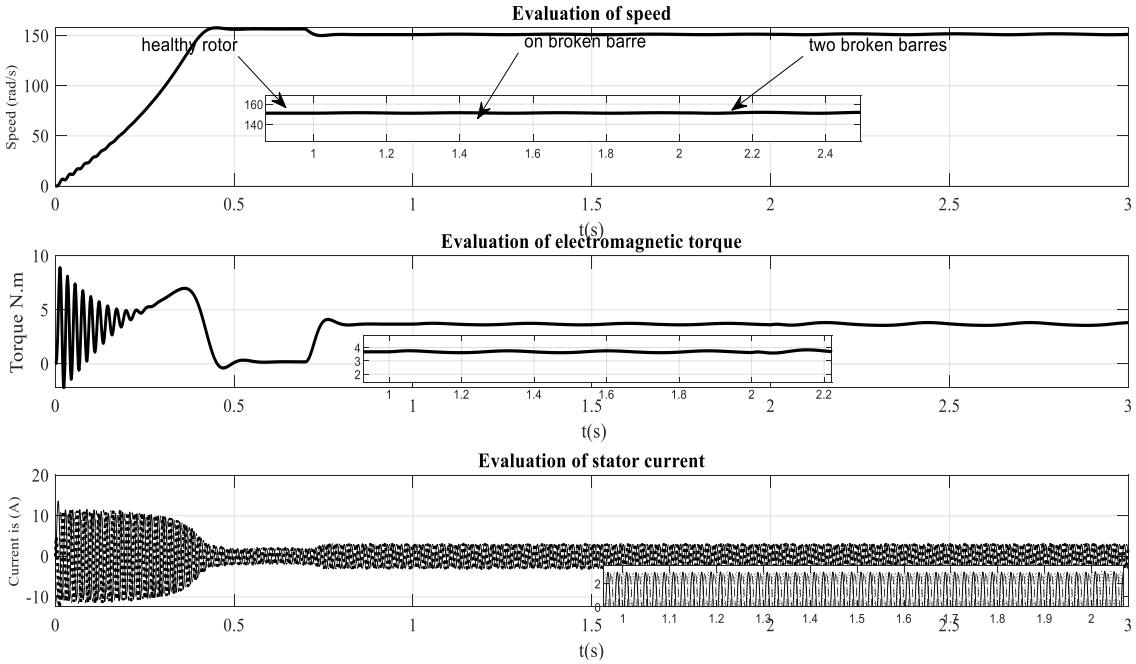

Figure 7. Speed, torque, and currents waveforms in the presence of rotor broken bars under load Tr = 3.5 N.m

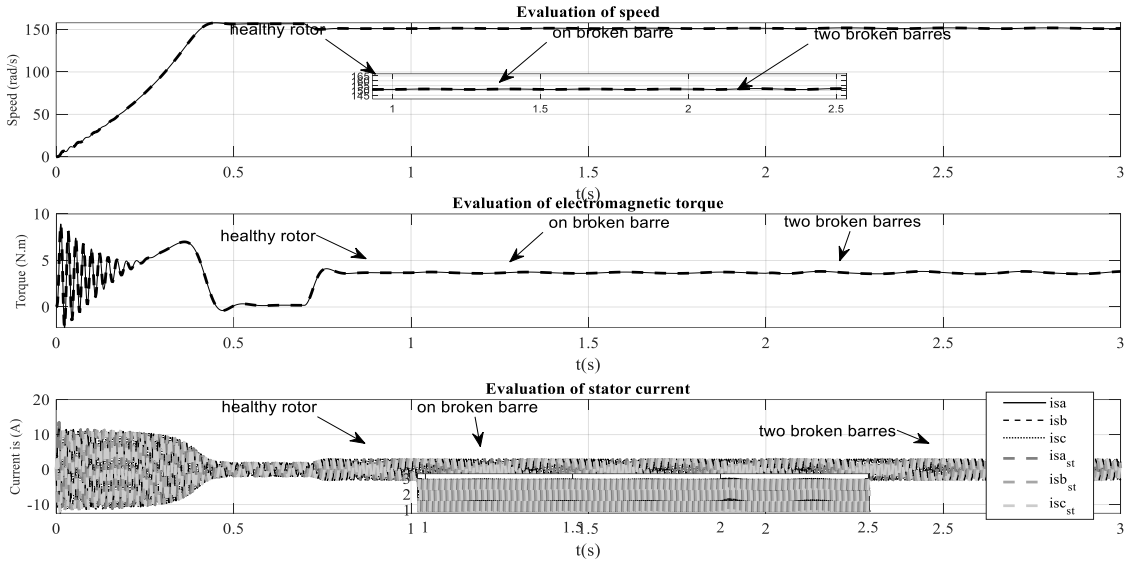

Figure 8. Speed, torque, and currents waveforms in the presence of rotor broken bars using TS models

4. RESULTS AND DISCUSSION

This section provides and discusses the simulation results of the classical models and Takagi–Sugeno-based models under healthy condition, single faults, and multi-fault conditions. The results determine the effect of every fault condition on the dynamic response of the motor, i.e., current asymmetries, torque disturbances, and speed variations. A comparative discussion is provided to evaluate the sufficiency of the proposed fuzzy modeling method compared to traditional methods in terms of accuracy, responsiveness, and usability for real-time diagnosis.

4.1. IM with simultaneous rotor and stator faults in the rotor frame

Since the two main faults of the IM can be decoupled, a general model of the IM is proposed in the case of the presence of simultaneous rotor and stator faults which can hamper the healthy operation of the machine (Park model). The fault of short circuits of turns affecting the stator (short-circuit quadruple) and the broken rotor bar through the fault resistance are simulated [21].

4.1.1. State-space representation of simultaneous faults

The model of the IM with stator/rotor faults is presented in (16) and (17). This formulation represents the behavior of the machine under fault conditions.

$$\begin{cases} \dot{x}(t) = A(\omega).x(t) + B(t).u(t) \\ y(t) = C.x(t) + D.u(t) \end{cases} \quad (16)$$

With:

$$A(\omega) = \begin{bmatrix} -\left([R_s] + [R_{eq}]\right).L_f^{-1} - \omega.P(\frac{\pi}{2}) & \left([R_{eq}].L_m^{-1} - \omega.P\left(\frac{\pi}{2}\right)\right).L_f^{-1} \\ [R_{eq}] & -[R_{eq}].L_m^{-1} \end{bmatrix}, B = \begin{bmatrix} \frac{1}{L_f} & 0 \\ 0 & \frac{1}{L_f} \\ 0 & 0 \\ 0 & 0 \end{bmatrix},$$

$$C = \begin{bmatrix} 1 & 0 & 0 & 0 \\ 0 & 1 & 0 & 0 \end{bmatrix}, D = \sum_{k=1}^{3} \frac{2}{3} \frac{n_{cck}}{R_s} P(-\theta) Q(\theta_{cck}) P(\theta) \quad (17)$$

4.1.2. Simulation results

The simulation of the model allows to obtain the evolution of the electromagnetic torque, the speed and the stator currents of the IM in the presence of simultaneous faults, where a breaking rotor bar fault is introduced in steady state at t = 1 s and the 32-turn short-circuit fault affecting phase as at time t = 2 s. Figure 9 shows the existence of large oscillations in the evolution of speed and electromagnetic torque. This leads to intense mechanical vibrations. The currents waveforms illustrated in Figure 9 show a significant increase in the current amplitude when the fault occurs (caused by the stator fault) accompanied by the presence of identical oscillations on the three currents (caused by the rotor fault). Simultaneous rotor and stator faults cause speed oscillations of ±20 rad/s, with corresponding torque oscillations up to 5 N.m.

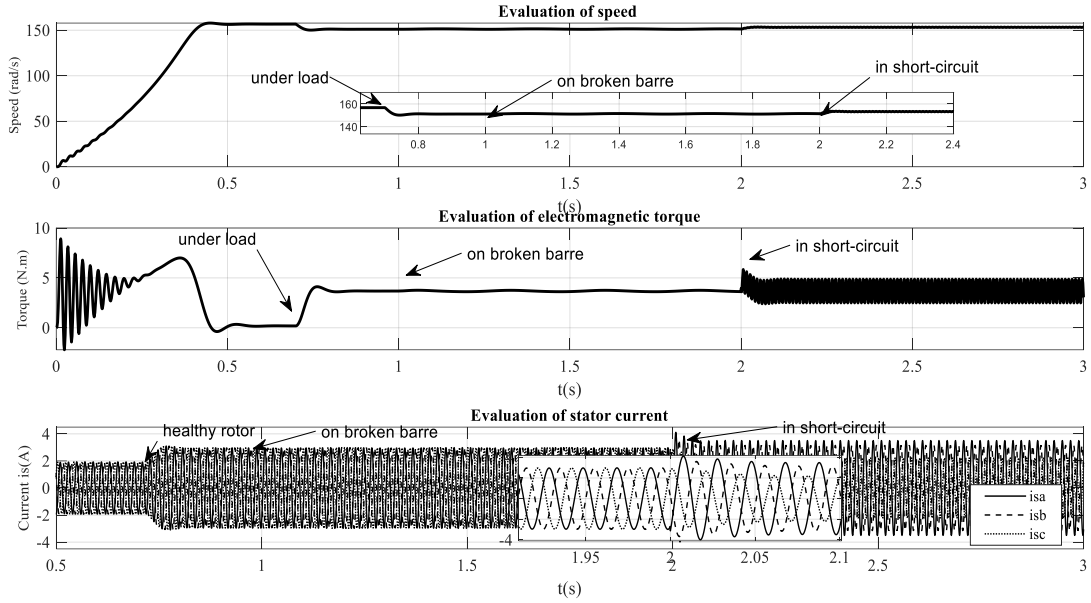

Figure 9. Speed, torque and currents waveforms in the presence of simultaneous rotor and stator faults

4.1.3. TS Model representation of simultaneous faults

As shown in (16), we notice that the matrices B and C in case of stator fault using TS representation are constants where, the matrix state A depend on the speed, which represents the only nonlinearity: $z(t) = \omega$. The matrices of the system are given as:

$$A_1 = \begin{bmatrix} -([R_s] + [R_{eq}]) \cdot L_f^{-1} - W.P\left(\frac{\pi}{2}\right) & \left([R_{eq}] \cdot L_m^{-1} - W.P\left(\frac{\pi}{2}\right)\right) \cdot L_f^{-1} \\ [R_{eq}] & -[R_{eq}] \cdot L_m^{-1} \end{bmatrix},$$

$$A_2 = \begin{bmatrix} -([R_s] + [R_{eq}]) \cdot L_f^{-1} - w.P\left(\frac{\pi}{2}\right) & \left([R_{eq}] \cdot L_m^{-1} - w.P\left(\frac{\pi}{2}\right)\right) \cdot L_f^{-1} \\ [R_{eq}] & -[R_{eq}] \cdot L_m^{-1} \end{bmatrix},$$

$$B_1 = B_2 = B, \quad C_1 = C_2 = C, \quad D_1 = D_2 = D.$$

4.1.4. Simulation results based on TS models

Figure 10 presents the Simulink block diagram used for the fault diagnosis simulations. Description of the Simulink model: This model is crucial for testing our hypotheses under controlled conditions, replicating real-world scenarios where motor faults occur. Here is a step-by-step explanation of the block diagram components:

i. Input signal block: generates the electrical signals mimicking those from an induction motor experiencing various faults.
ii. Fault insertion module: simulates specific faults by altering signal characteristics such as amplitude and phase. This module allows the injection of predefined faults such as rotor bar breaks or stator short circuits.
iii. Takagi-Sugeno Fuzzy model block: processes the input signals through a fuzzy logic system to estimate the fault severity and type. This block uses sets of rules derived from the motor's typical response patterns to detect anomalies.
iv. Data processing unit: analyzes the output from the fuzzy model, comparing it with expected normal operation parameters to quantify the deviation caused by faults.
v. Output analysis block: visualizes the results in a form that can be easily interpreted, showing key diagnostic metrics such as fault severity and location.

Each component is parameterized based on the motor specifications, including resistance, inductance, and operational voltages, ensuring that the simulations reflect realistic operating conditions. The results generated from this model provide a clear interpretation of how different faults impact motor performance, facilitating effective diagnosis.

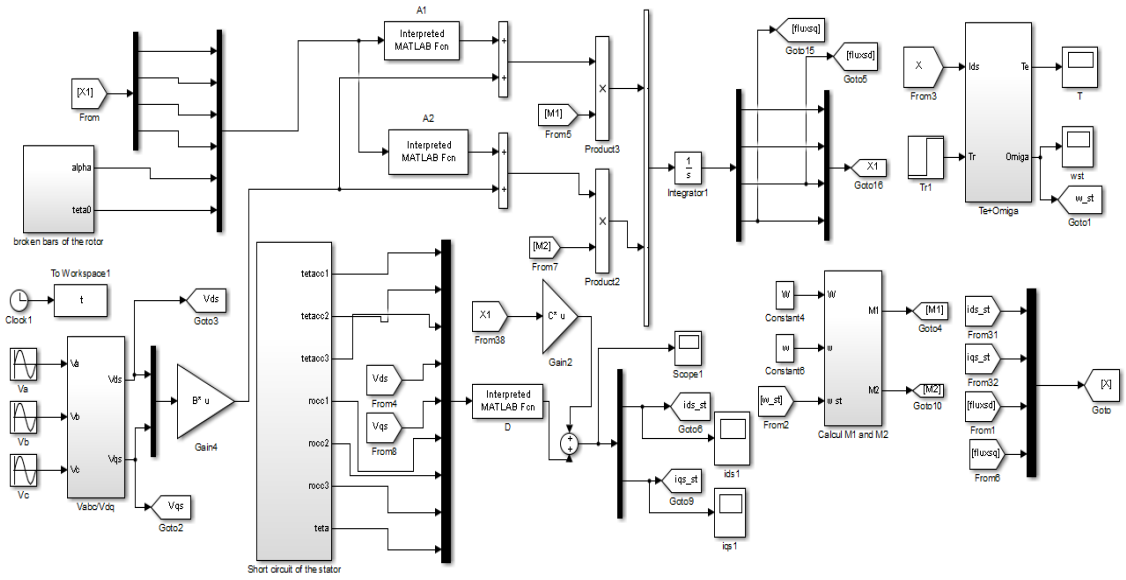

Figure 10. Simultaneous stator and rotor faults model based on T-S approach under MATLAB/Simulink

Impact of neglecting inductance changes: After illustrating the efficiency of our TS model-based diagnostic approach, as shown in Figure 10, it is critical to address the simplifications inherent in our model, particularly our focus on resistance changes without equally considering inductance variations. In our study, we primarily considered resistance changes to model the induction motor faults. However, this subsection addresses the potential implications of this assumption. Inductance changes can play a critical role, particularly in scenarios involving severe faults or under specific operational conditions such as high load or variable frequency drives. The potential impacts of neglecting inductance changes include: misdiagnosis of fault types. Inductance variations can mask or mimic resistance changes, leading to incorrect fault identification. Accuracy of fault severity: Inaccurate fault severity assessment can result from not accounting for inductance changes, particularly in complex motor configurations. Guidelines for neglecting inductance changes:

- Minor faults: for minor faults where changes are primarily resistive, and motor operation remains stable, neglecting inductance changes is acceptable.
- Severe faults: in cases of severe faults or where the motor performance is critically degraded, both resistance and inductance should be considered to ensure accurate diagnostics.

The obtained results of speed, torque and currents have been shown in Figure 11. Simultaneous faults result in torque oscillations reaching up to 5.5 N.m and speed variations of ±25 rad/s. The currents increase in amplitude to approximately 6 A during fault conditions.

4.1.5. Discussion

The simulation results for the stator, rotor, and mixed faults agree with the success of the developed Takagi–Sugeno (TS) fuzzy model in fault modeling and diagnosis of induction motors. Unlike conventional techniques relying on linear behavior assumptions or competing solely on current signatures, the TS model offers a robust description of the dynamic motor response under faults. Particularly, the model attains fault-induced disturbances in torque and speed, which are masked during transient regimes. The same is particularly crucial in the diagnosis of faults that appear simultaneously, where the superposition of symptoms obscures fault patterns in traditional models. The escalation of torque ripple and speed oscillations observed in simultaneous fault conditions similarly accentuates the diagnostic sensitivity of our method.

Compared to other work done for fault injection into stator or rotor separately, our holistic framework offers modularity in fault injection and scalable diagnostics. Our framework does not require retraining or offline tuning for significant time, which makes it suitable for embedded real-time systems. In practice, the diagnostic and modeling paradigm can be integrated in predictive maintenance software to reduce downtime and maintenance cost. Experimental verification on a test bench and exploration of real-time hardware-in-the-loop implementations will be considered as future work to validate robustness with noisy data and parameter drift.

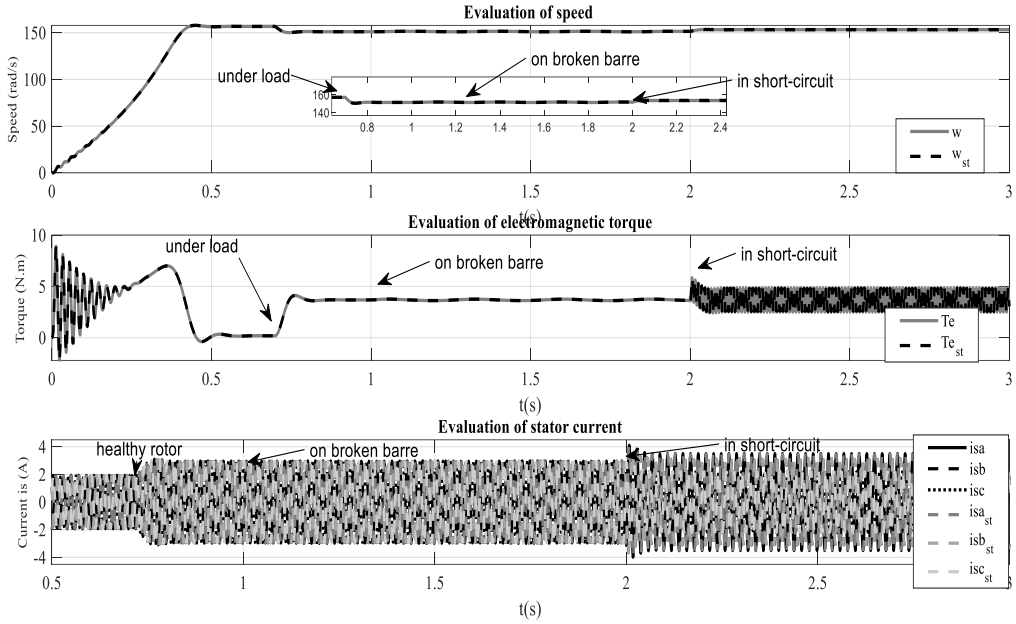

Figure 11. Speed, torque, and currents quantities based TS models under load T_r = 3.5 N.m in the presence of simultaneous faults

5. CONCLUSION

In this paper, a new approach based on Takagi–Sugeno (TS) models has been presented to model and detect various faults of induction motors (IMs), e.g., stator faults, rotor faults, and overall stator–rotor faults. The approach has been validated with simulation results and demonstrates stable performance under dynamic and transient modes of operation. The proposed approach is extremely robust and flexible in fault detection and discrimination among different fault conditions using only electrical quantities, rendering it an appropriate choice for industrial practice. The work's main contributions are the development of a unified TS model-based fault diagnosis scheme applicable to healthy and faulty IMs, accurate modeling of fault dynamics in the rotor reference frame, and the demonstration of the effectiveness of the method under multiple fault conditions. For future work, we plan to implement the proposed diagnostic system on real-time hardware using embedded platforms in order to validate its performance under realistic operating conditions. Further, generalization of the approach to fault severity estimation and diagnosis with noisy measurements or faulty sensors will be investigated to further expand its industrial use.

FUNDING INFORMATION

The authors state that no funding was received for this research.

AUTHOR CONTRIBUTIONS STATEMENT

This journal uses the Contributor Roles Taxonomy (CRediT) to recognize individual author contributions, reduce authorship disputes, and facilitate collaboration.

Name of Author	C	M	So	Va	Fo	I	R	D	O	E	Vi	Su	P	Fu
Samira Souri	✓	✓	✓	✓	✓	✓		✓	✓	✓	✓	✓	✓	
Mohamed Lakhdar Louazene		✓		✓	✓	✓	✓			✓		✓		
Abdelghani Djeddi				✓	✓	✓				✓	✓			
Youcef Soufi				✓		✓				✓		✓		

C : **C**onceptualization
M : **M**ethodology
So : **So**ftware
Va : **Va**lidation
Fo : **Fo**rmal analysis
I : **I**nvestigation
R : **R**esources
D : **D**ata Curation
O : Writing - **O**riginal Draft
E : Writing - Review & **E**diting
Vi : **Vi**sualization
Su : **Su**pervision
P : **P**roject administration
Fu : **Fu**nding acquisition

CONFLICT OF INTEREST STATEMENT

The authors declare no conflict of interest.

DATA AVAILABILITY

The data supporting the findings of this study are fully presented within the article. Additional information or further details can be obtained from the corresponding author upon reasonable request.

REFERENCES

[1] M. Messaoudi, A. Flah, A. A. Alotaibi, A. Althobaiti, L. Sbita, and C. Z. El-Bayeh, "Diagnosis and fault detection of rotor bars in squirrel cage induction motors using combined Park's vector and extended Park's vector approaches," *Electronics*, vol. 11, no. 3, p. 380, Jan. 2022, doi: 10.3390/electronics11030380.

[2] M. E. H. Benbouzid, "A review of induction motors signature analysis as a medium for faults detection," *IEEE Transactions on Industrial Electronics*, vol. 47, no. 5, pp. 984–993, 2000, doi: 10.1109/41.873206.

[3] R. Kechida, A. Menacer, and H. Cherif, "Broken rotor bars fault detection in induction motors using FFT: simulation and experimentally study," *Algerian Journal of Engineering and Technology*, vol. 1, pp. 19–24, 2019.

[4] O. E. Hassan, M. Amer, A. K. Abdelsalam, and B. W. Williams, "Induction motor broken rotor bar fault detection techniques based on fault signature analysis – a review," *IET Electric Power Applications*, vol. 12, no. 7, pp. 895–907, Aug. 2018, doi: 10.1049/iet-epa.2018.0054.

[5] A. Siddique, G. S. Yadava, and B. Singh, "A review of stator fault monitoring techniques of induction motors," *IEEE Transactions on Energy Conversion*, vol. 20, no. 1, pp. 106–114, Mar. 2005, doi: 10.1109/TEC.2004.837304.

[6] S. K. Ramu, G. C. R. Irudayaraj, S. Subramani, and U. Subramaniam, "Broken rotor bar fault detection using Hilbert transform and neural networks applied to direct torque control of induction motor drive," *IET Power Electronics*, vol. 13, no. 15, pp. 3328–3338, Nov. 2020, doi: 10.1049/iet-pel.2019.1543.

[7] B. H. Bahgat, E. A. Elhay, and M. M. Elkholy, "Advanced fault detection technique of three phase induction motor: comprehensive review," *Discover Electronics*, vol. 1, no. 1, p. 9, Jun. 2024, doi: 10.1007/s44291-024-00012-3.

[8] X. Qu, B. Duan, Q. Yin, M. Shen, and Y. Yan, "Deep convolution neural network based fault detection and identification for modular multilevel converters," in *2018 IEEE Power & Energy Society General Meeting (PESGM)*, IEEE, Aug. 2018, pp. 1–5, doi: 10.1109/PESGM.2018.8586661.

[9] N. Batra, A. Singh, and K. Whitehouse, "If you measure it, can you improve it? Exploring the value of energy disaggregation," in *Proceedings of the 2nd ACM International Conference on Embedded Systems for Energy-Efficient Built Environments*, New York, NY, USA: ACM, Nov. 2015, pp. 191–200, doi: 10.1145/2821650.2821660.

[10] Y. S. Wang, Q. H. Ma, Q. Zhu, X. T. Liu, and L. H. Zhao, "An intelligent approach for engine fault diagnosis based on Hilbert–Huang transform and support vector machine," *Applied Acoustics*, vol. 75, pp. 1–9, Jan. 2014, doi: 10.1016/j.apacoust.2013.07.001.

[11] P. Vas, *Sensorless Vector and Direct Torque Control*. Oxford, U.K: Oxford University Press, 1998, doi: 10.1093/oso/9780198564652.001.0001.

[12] B. K. Bose, *Modern Power Electronics and AC Drives*. Upper Saddle River, NJ, USA: Prentice Hall, 2002.

[13] B. Lu, T. G. Habetler, and R. G. Harley, "A survey of efficiency-estimation methods for in-service induction motors," *IEEE Transactions on Industry Applications*, vol. 42, no. 4, pp. 924–933, Jul. 2006, doi: 10.1109/TIA.2006.876065.

[14] K. Ouarid, M. Essabre, A. El Assoudi, and E. H. El Yaagoubi, "State and fault estimation based on fuzzy observer for a class of Takagi-Sugeno singular models," *Indonesian Journal of Electrical Engineering and Computer Science*, vol. 25, no. 1, pp. 172–182, Jan. 2022, doi: 10.11591/ijeecs.v25.i1.pp172-182.

[15] K. Aitdaraou, M. Essabre, A. El Assoudi, and E. H. El Yaagoubi, "A fuzzy observer synthesis to state and fault estimation for Takagi-Sugeno implicit systems," *IAES International Journal of Artificial Intelligence (IJ-AI)*, vol. 12, no. 1, pp. 241–250, Mar. 2023, doi: 10.11591/ijai.v12.i1.pp241-250.

[16] M. Sugeno and K. Tanaka, "Successive identification of a fuzzy model and its applications to prediction of a complex system," *Fuzzy Sets and Systems*, vol. 42, no. 3, pp. 315–334, Aug. 1991, doi: 10.1016/0165-0114(91)90110-C.

[17] M. N. Uddin, T. S. Radwan, and M. A. Rahman, "Performances of fuzzy-logic-based indirect vector control for induction motor drive," *IEEE Transactions on Industry Applications*, vol. 38, no. 5, pp. 1219–1225, Sep. 2002, doi: 10.1109/TIA.2002.802990.

[18] J. Pan, A.-T. Nguyen, T.-M. Guerra, C. Sentouh, S. Wang, and J.-C. Popieul, "Vehicle actuator fault detection with finite-frequency specifications via Takagi-Sugeno fuzzy observers: theory and experiments," *IEEE Transactions on Vehicular Technology*, vol. 72, no. 1, pp. 407–417, Jan. 2023, doi: 10.1109/TVT.2022.3204326.

[19] S. Nandi, H. A. Toliyat, and X. Li, "Condition monitoring and fault diagnosis of electrical motors—a review," *IEEE Transactions on Energy Conversion*, vol. 20, no. 4, pp. 719–729, Dec. 2005, doi: 10.1109/TEC.2005.847955.

[20] A. Bellini, F. Filippetti, C. Tassoni, and G.-A. Capolino, "Advances in diagnostic techniques for induction machines," *IEEE Transactions on Industrial Electronics*, vol. 55, no. 12, pp. 4109–4126, Dec. 2008, doi: 10.1109/TIE.2008.2007527.

[21] D. Yarymbash, S. Yarymbash, M. Kotsur, and T. Divchuk, "Enhancing the effectiveness of calculation of parameters for short circuit of threephase transformers using field simulation methods," *Eastern-European Journal of Enterprise Technologies*, vol. 4, no. 5 (94), pp. 22–28, Aug. 2018, doi: 10.15587/1729-4061.2018.140236.

[22] M. E. H. Benbouzid and G. B. Kliman, "What stator current processing-based technique to use for induction motor rotor faults diagnosis?," *IEEE Transactions on Energy Conversion*, vol. 18, no. 2, pp. 238–244, Jun. 2003, doi: 10.1109/TEC.2003.811741.

[23] J. Rengifo, J. Moreira, F. Vaca-Urbano, and M. S. Alvarez-Alvarado, "Detection of inter-turn short circuits in induction motors using the current space vector and machine learning classifiers," *Energies*, vol. 17, no. 10, p. 2241, May 2024, doi: 10.3390/en17102241.

[24] A. H. Bonnett and G. C. Soukup, "Cause and analysis of stator and rotor failures in three-phase squirrel-cage induction motors," *IEEE Transactions on Industry Applications*, vol. 28, no. 4, pp. 921–937, 1992, doi: 10.1109/28.148460.

[25] J. Chen and R. J. Patton, *Robust Model-Based Fault Diagnosis for Dynamic Systems*. Boston, MA: Springer US, 1999, doi: 10.1007/978-1-4615-5149-2.

[26] R. R. Schoen, T. G. Habetler, F. Kamran, and R. G. Bartfield, "Motor bearing damage detection using stator current monitoring," *IEEE Transactions on Industry Applications*, vol. 31, no. 6, pp. 1274–1279, 1995, doi: 10.1109/28.475697.

BIOGRAPHIES OF AUTHORS

Samira Souri is an assistant professor in the Department of Electronics and Telecommunications, Faculty of New Information Technologies and Communication, University Kasdi Merbah-Ouargla, Algeria. She obtained a master's degree in electrical engineering in 2006 from Mohamed Khider University, Biskra. Her research interests include modeling and control of nonlinear systems, fault detection and isolation in industrial processes, and intelligent systems based on fuzzy logic. She can be contacted at email: souri.samira@univ-ouargla.dz.

Mohamed Lakhdar Louazene is a professor in the Department of Electrical Engineering, Ouargla University. He was born in Ouargla, Algeria, in December 1967. He received an engineering degree in electrical engineering (1991), magister in renewable energy (2008) from the Electrical Engineering Institute of Batna University, Ph.D. degree in 2015 from Batna University, and his HDR in 2017 in electrical engineering from Ouargla University, Algeria. His principal research interests include photovoltaic water pumping systems and applications. He can be contacted at email: louazene.lakhdar@univ-ouargla.dz.

Abdelghani Djeddi is a professor of electrical engineering at the Department of Electrical Engineering, Faculty of Science and Technology, University of Tebessa. Prior to this, he served in the same capacity at Kasdi Merbah University, Ouargla, Algeria. He received his Ph.D. in electrical engineering in 2017 from Badji Mokhtar University of Annaba and later obtained his Habilitation à Diriger des Recherches (HDR) from Echahid Cheikh Larbi Tebessi University of Tebessa. His research interests span fractional calculus, modeling and control of nonlinear systems, fault detection and isolation in industrial processes, reliability engineering, and intelligent systems based on fuzzy logic. He can be contacted at email: abdelghani.djeddi@univ-tebessa.dz.

Youcef Soufi received the B.Eng. (1991) and doctorate degrees from the University of Annaba, Algeria, in electrical engineering. Since 2000, he has been with the Department of Electrical Engineering, Laboratory of Electrical Engineering at Echahid Larbi Tebessi University, Tebessa, Algeria. He is currently a full professor in electrical engineering. His main and current major research interests include smart grids, renewable energy, electrical machines control, power electronics, and drives. He has published and co-authored more than 200 technical papers in scientific journals and conference proceedings since 2000. He is a member of the editorial board of many journals, and a member of the technical program committee/international advisory board/international steering committee of many international conferences. He can be contacted at email: youcef.soufi@univ-tebessa.dz.